

Quartic-Scaling Analytical Gradient of Quasidegenerate Scaled Opposite Spin Second-Order Perturbation Corrections to Single Excitation Configuration Interaction

Young Min Rhee,[†] David Casanova, and Martin Head-Gordon*

Department of Chemistry, University of California, Berkeley, California 94720, and
Chemical Sciences Division, Lawrence Berkeley National Laboratory,
Berkeley, California 94720

Received November 25, 2008

Abstract: Quasidegenerate scaled second-order perturbation correction to single excitation configuration interaction (SOS-CIS(D₀)) is a viable method that can describe excited-state potential energy surfaces of various chemical systems both reliably and efficiently [*J. Chem. Phys.* **2008**, *128*, 164106]. In this work, its analytical gradient theory is developed and implemented into an efficient quartic-scaling algorithm. This low order scaling, as opposed to the traditional quintic scaling of various second-order perturbation methods, is attained by using the resolution-of-the-identity approximation and the Laplace transform. The efficiency of the method is demonstrated by calculating the excited-state gradients of molecules with varying sizes. The proposed gradient method will thus be useful in studying various chemical systems, ranging from finding the optimized stable geometry on the excited surface to elucidating interesting excited-state dynamics around the avoided crossing region.

I. Introduction

Obtaining an efficient and reliable theory for describing electronically excited states has been a long-standing research theme for many quantum chemists over many decades. For developing theories that can describe excitations from single-reference ground states, there have been a number of branches of endeavors: designing more reliable correction schemes for single excitation configuration interaction (CIS),¹ implementing linear response^{2–4} or equation-of-motion theory^{5,6} for various levels of coupled-cluster (CC)⁷ expansions, and trying to eliminate errors in exchange-correlation description for the formally accurate time-dependent density functional theory (TDDFT).^{8,9} Of these three branches, the correction scheme on CIS and the linear response scheme on truncated CC have much in common, primarily because they are both wave function-based theories.

In fact, developing efficient and reliable wave function-based excited-state theories is entering into a Renaissance in recent

years. Of course, this is in part due to the advance of high performance computational platforms, where more costly calculations with wave function-based methods can be executed with a relative ease. However, recent endeavors in designing new algorithms and quantum chemical models and the subsequent successes have been the more important driving force for the changes. For example, the resolution-of-the-identity (RI) approximation,^{10–15} which uses the density fitting^{16–18} formulation by auxiliary basis expansion, has been widely adopted in recent developments, because it significantly reduces the computational cost associated with transforming various atomic orbital (AO) based electron repulsion integrals into molecular orbital (MO) based ones. Another important development has been the application of the Laplace transform algorithm proposed by Almlöf and co-workers.^{19,20} Through this application, Scuseria and co-workers have shown that the traditional fifth-order scaling Møller–Plesset second-order perturbation scheme (MP2)²¹ can be rendered into a linear scaling algorithm when applied to large enough molecular systems.²² They have also shown that the MP2 theory can be efficiently applied to periodic systems through the use of the Laplace transform real-space formulation.²³ Furthermore, the RI and the Laplace

* Corresponding author e-mail: mhg@cchem.berkeley.edu.

[†] Present address: Department of Chemistry, Pohang University of Science and Technology, Pohang 790-784, Korea.

transform techniques have been recently combined to improve the efficiencies of the local MP2 model²⁴ and of the MP2 scheme for periodic systems.²⁵ It is also interesting to note the development of the spin component scaling (SCS) concept, which was pioneered by Grimme and co-workers^{26,27} and rigorously interpreted by Szabados.²⁸ Relevant to the present work, Head-Gordon and co-workers have shown that the scaled opposite spin (SOS) version of perturbative corrections can improve the accuracy of both ground-state theory²⁹ (MP2) and excited-state theory³⁰ (perturbative doubles corrections for CIS; CIS(D)³¹). A similar behavior was also reported³² for the quasidegenerate development of the perturbative correction scheme, CIS(D₀).³³ Hättig and co-workers have also reported³⁴ similar improvements in the robustness of truncated coupled-cluster theory CC2³⁵ through the use of these SCS and SOS approaches.

Among the above two scaling approaches, the SOS implementation has an important advantage: its computational demands for energy calculations only scale as fourth-order with respect to the molecular size when it is combined with the above-mentioned RI and Laplace transform techniques.^{29,30,32} Achieving this scaling property, which is formally similar to the cost of mean field approaches such as CIS or TDDFT, is an important development because it allows us to apply the new methods to the calculation of much larger systems than what is practically feasible with conventional fifth-order scaling CIS(D)/CC2 or their SCS variants. In the same sense, attaining a similar efficiency in calculating the corresponding analytical gradient of the method will also be important, as the gradient is used in various situations of quantum chemical studies. In fact, for the ground-state SOS theory (SOS-MP2), it is already proven that such an efficient calculation is actually possible.³⁶

In this work, we derive the analytical gradient of the fourth-order scaling quasidegenerate excited-state theory SOS-CIS(D₀). We prove that its gradient can also be obtained with a fourth-order scaling computational effort and propose an efficient algorithm for its actual computation. Then we apply the algorithm to various molecular systems and demonstrate that the gradient can actually be obtained very efficiently. The efficiency is shown to be strikingly good when it is compared with the case of the analytic gradient of the sister ground-state theory, SOS-MP2. As SOS-CIS(D₀) is an efficient and appropriate method for describing excited-state potential energy surfaces even near degeneracies, and as it does not suffer from the notorious problem for describing charge transfer excitations as in conventional TDDFT,^{37–43} we expect that this gradient implementation will be useful in studying various chemical systems in their electronic excitations. Such an aspect is also discussed as a conclusion of this article.

II. Theory

In this section we will describe the formulation of the analytical gradient of SOS-CIS(D₀) theory, whose energy expression is given as^{32,33}

$$\omega = \mathbf{b} \mathbf{A}_{\text{SS}}^{(0)} \mathbf{b} + c_T \mathbf{b} \mathbf{A}_{\text{SS}}^{(2)} \mathbf{b} + c_U \mathbf{b} \mathbf{A}_{\text{SD}}^{(1)} [\mathbf{D}_{\text{DD}}^{(0)}]^{-1} \mathbf{A}_{\text{DS}}^{(1)} \mathbf{b} \quad (1)$$

When we define the system Hamiltonian and its first-order fluctuation potential as \hat{H} and \hat{V} , the response matrix elements can be expressed as

$$\mathbf{A}_{\text{SS}}^{(0)} = \langle \Phi_S | \hat{H} | \Phi_S \rangle \quad (2)$$

$$\mathbf{A}_{\text{SS}}^{(2)} = \langle \Phi_S | \hat{V} | \hat{T}_2^{\text{OS}} \Phi_S \rangle \quad (3)$$

$$\mathbf{A}_{\text{SD}}^{(1)} = \langle \Phi_S | \hat{V} | \Phi_D^{\text{OS}} \rangle \quad (4)$$

together with the well-known Møller–Plesset excitation operator \hat{T}_2^{OS} in the opposite spin space. Here Φ_S represents a Slater determinant singly excited from the ground configuration Φ_0 , while Φ_D^{OS} represents a determinant doubly excited in the opposite spin space. The expression for $\mathbf{A}_{\text{DS}}^{(1)}$ is obvious from eq 4, and the zeroth-order DD block is the diagonal eigenvalue difference matrix $\varepsilon_a + \varepsilon_b - \varepsilon_i - \varepsilon_j$. In addition, \mathbf{b} represents the vector with single excitation amplitudes which is obtained as the eigenvector of the entire response matrix, $\mathbf{A}_{\text{SS}}^{(0)} + c_T \mathbf{A}_{\text{SS}}^{(2)} + c_U \mathbf{A}_{\text{SD}}^{(1)} [\mathbf{D}_{\text{DD}}^{(0)}]^{-1} \mathbf{A}_{\text{DS}}^{(1)}$. Finally, c_T and c_U represent the opposite spin component scaling parameters as defined previously.^{30,32}

For future references, let us define the three terms on the right-hand side of eq 1 as ω_0 , ω_T , and ω_U , respectively

$$\omega = \omega_0 + \omega_T + \omega_U \quad (5)$$

Of the three, ω_0 requires only fourth-order scaling contractions between $\mathbf{A}_{\text{SS}}^{(0)}$ and \mathbf{b} , and we will use exact integrals without any approximations for this term. This is similar to the case of evaluating electron repulsion integrals (ERIs) in Hartree–Fock (HF) self-consistent field (SCF) solution, where exact integrals are used without the RI approximation. For ω_T and ω_U , ERIs are evaluated with the RI approximation^{10–16,44}

$$(pq|rs)_{\text{RI}} = \sum_{PQ} (pq|P)(P|Q)^{-1}(Q|rs) = \sum_R B_{pq}^R B_{rs}^R \quad (6)$$

with the \mathbf{B} matrix defined as

$$B_{pq}^R = \sum_P (pq|P)(P|R)^{-1/2} \quad (7)$$

together with an auxiliary basis set $\{P\}$. With the above explanation, one can easily infer where RI approximations are adopted, and we will not explicitly use the subscript “RI” in the following equations for the sake of simplicity.

Because \mathbf{b} is obtained as the eigenvector of the symmetrized response matrix,³² the first derivative of ω with respect to some parameter x can be obtained as

$$\omega^{(x)} = \mathbf{b} [\mathbf{A}_{\text{SS}}^{(0)}]^{(x)} \mathbf{b} + c_T \mathbf{b} [\mathbf{A}_{\text{SS}}^{(2)}]^{(x)} \mathbf{b} + c_U \mathbf{b} [\mathbf{A}_{\text{SD}}^{(1)} (\mathbf{D}_{\text{DD}}^{(0)})^{-1} \mathbf{A}_{\text{DS}}^{(1)}]^{(x)} \mathbf{b} \quad (8)$$

The gradient expression originating from ω_0 term is identical to the CIS case, and readers are referred to the detailed derivations in refs 45 and 46.

As in the case of the sister ground-state theory SOS-MP2, the quartic-scaling SOS-CIS(D₀) utilizes the Laplace transform of the energy denominator^{19,29,30,32}

$$\frac{1}{\Delta_{ij}^{ab}} = \sum_t \rho_t \exp(-\Delta_{ij}^{ab} t) \quad (9)$$

with ρ_t denoting the weight at any given quadrature point t , and Δ representing the diagonal energy difference tensor $\Delta_{ij}^{ab} = \varepsilon_a + \varepsilon_b - \varepsilon_i - \varepsilon_j$. Therefore, to obtain the expression of the

analytical gradient of both SOS-MP2 and SOS-CIS(D₀), one needs to derive the first derivative of $e^{-\Delta t}$. Because a tensor Δ and its derivative $\Delta^{(x)}$ do not commute unless both are diagonal, the following simple formulation is not generally satisfied

$$[e^{-\Delta t}]^{(x)} \neq -te^{-\Delta t}\Delta^{(x)} \quad (10)$$

One approach to satisfy the above equality is to restrict the orbitals to be canonical by setting the Fock matrix ε_{pq} diagonal even after the perturbation “ χ ”⁴⁷

$$\varepsilon_{pq}^{(x)} = \varepsilon_{pq}^{(x)}\delta_{pq} \quad (11)$$

Indeed, Lochan et al. developed the quartic-scaling SOS-MP2 gradient theory through the use of this canonical representation.³⁶

Even though $\Delta^{(x)}$ may not be diagonal in general, we should note from Brillouin’s theorem that it is still block-diagonal.⁴⁸ In fact, as long as Δ is diagonal and $\Delta^{(x)}$ is block-diagonal, one can show that the following equation is satisfied (see the Appendix for its detailed proof)

$$[e^{-\Delta t}]_{ijab;i'j'a'b'}^{(x)} = -t\varepsilon_{aa}^{(x)}\delta_{ii'}\delta_{jj'}\delta_{bb'}e^{-\Delta_{ij}^{(x)}t}h(\Delta_{a't}^{(x)}) - t\varepsilon_{bb}^{(x)}\delta_{ii'}\delta_{jj'}\delta_{aa'}e^{-\Delta_{ij}^{(x)}t}h(\Delta_{b't}^{(x)}) + t\varepsilon_{ii'}^{(x)}\delta_{ii'}\delta_{aa}\delta_{bb}e^{-\Delta_{ij}^{(x)}t}h(\Delta_{i't}^{(x)}) + t\varepsilon_{jj'}^{(x)}\delta_{ii'}\delta_{aa}\delta_{bb}e^{-\Delta_{ij}^{(x)}t}h(\Delta_{j't}^{(x)}) \quad (12)$$

with $h(x) = (1 - e^{-x})/x$ and $\Delta_p^q = \varepsilon_q - \varepsilon_p$. With this more generalized equation for $\Delta^{(x)}$, one can use the symmetric representation of the occupied-occupied and virtual-virtual orbital responses^{49,50}

$$U_{ij}^x = -\frac{1}{2}S_{ij}^x \quad (13a)$$

$$U_{ab}^x = -\frac{1}{2}S_{ab}^x \quad (13b)$$

where the S^x matrices correspond to the derivatives of the overlap integrals. Curious readers can rederive SOS-MP2 gradient using this symmetric representation and can show that the final expressions are identical to the ones obtained with the canonical representation. Besides this interesting complementary nature, the benefit of using the symmetric representation presented here is the associated simplicity in the derivation of the analytical gradient. Accordingly, we will exclusively use the symmetric representation in conjunction with eq 12.

A. Gradient from ω_T Term. In this section we derive the expression for the analytical gradient of the second term in eq 1. Following the conventional orbital designations³⁰ (i, j, \dots for occupied; a, b, \dots for virtual; overbar for β -spin), the detailed expression for this term can be given as

$$\begin{aligned} \omega_T = & -a_{jk}^{bc}b_i^ab_j^b(\bar{j}\bar{a}|kc) - a_{jk}^{bc}b_i^ab_j^b(\bar{i}\bar{b}|kc) + \\ & a_{jk}^{bc}b_i^ab_j^b(ik|lac) + a_{jk}^{bc}b_i^ab_j^b(\bar{i}\bar{a}|kc) - \\ & a_{jk}^{bc}b_i^ab_j^b(ja|l\bar{k}\bar{c}) - a_{jk}^{bc}b_i^ab_j^b(ib|l\bar{k}\bar{c}) + \\ & a_{jk}^{bc}b_i^ab_j^b(\bar{i}\bar{k}|l\bar{a}\bar{c}) + a_{jk}^{bc}b_i^ab_j^b(ial\bar{k}\bar{c}) \quad (14) \end{aligned}$$

Because the closed-shell expression can be easily obtained from this general spin-unrestricted description by setting $b_i^a = b_i^a$ ($b_i^a = -b_i^a$) for singlet (triplet) excitations, we will only present

the spin-unrestricted equations. By applying eq 12, the gradient of its first term can be formulated as

$$\begin{aligned} [-a_{jk}^{bc}b_i^ab_j^b(\bar{j}\bar{a}|kc)]^{(x)} = & \sum_t \rho_t [(\bar{j}\bar{b}|kc)^{(x)} \bar{W}_{bj}^Q \bar{B}_{ck}^Q + \bar{B}_{bj}^P \bar{B}_{ck}^P P_{ab}^P (\bar{j}\bar{a}|kc)^{(x)}] + \\ & \sum_t \rho_t P_{ab}^P (\bar{j}\bar{a}|kc) [-\varepsilon_{ba}^{(x)} \exp(-\Delta_{jk}^{(x)}t) \bar{h}_d^b t(\bar{j}\bar{d}|kc) - \\ & \varepsilon_{cd}^{(x)} \exp(-\Delta_{jk}^{(x)}t) \bar{h}_d^c t(\bar{j}\bar{b}|kd) + \varepsilon_{jl}^{(x)} \exp(-\Delta_{jk}^{(x)}t) \bar{h}_d^l t(\bar{j}\bar{d}|lc) + \\ & \varepsilon_{kl}^{(x)} \exp(-\Delta_{jk}^{(x)}t) \bar{h}_d^l t(\bar{j}\bar{b}|lc)] \quad (15) \end{aligned}$$

Because $\mathbf{b}^{(x)}$ does not appear in the overall derivative of the SOS-CIS(D₀) energy according to eq 8, we can safely omit any terms involving $\mathbf{b}^{(x)}$. The dot over the equality sign in the above equation explicitly remarks this omission. In reaching eq 15, we have used the definition

$$\bar{h}_p^q = h(\Delta_p^q) = \frac{1 - e^{-\Delta_p^q t}}{\Delta_p^q t} \quad (16)$$

together with its index exchange property given as

$$\bar{h}_q^p = \bar{h}_p^q e^{-\Delta_p^q t} \quad (17)$$

The definitions of other intermediates adopted in eq 15 and any subsequent equations can be found in Table 1.

The derivatives of the remaining terms from eq 14 can be obtained in a similar fashion. After some algebra, the analytical gradient of ω_T can be expressed in a rather compact form

$$\begin{aligned} [\omega_T]^{(x)} = & 2\Pi_{ai}^P (ai|P)^x + 2\Pi_{ai}^P (\bar{a}\bar{i}|P)^x - \gamma_{RS}^\Pi (R|S)^x + \\ & W_{ab}^\Pi S_{ab}^x + W_{ab}^\Pi S_{ab}^x + 2W_{ai}^\Pi S_{ai}^x + 2W_{ai}^\Pi S_{ai}^x + W_{ij}^\Pi S_{ij}^x + \\ & W_{ij}^\Pi S_{ij}^x + 2L_{ai}^\Pi U_{ai}^x + 2L_{ai}^\Pi U_{ai}^x + P_{ab}^\Pi \varepsilon_{ab}^{(x)} + P_{ab}^\Pi \varepsilon_{ab}^{(x)} + \\ & P_{ij}^\Pi \varepsilon_{ij}^{(x)} + P_{ij}^\Pi \varepsilon_{ij}^{(x)} \quad (18) \end{aligned}$$

with $(ai|P)^x$ denoting the atomic orbital derivative of the 3-centered 2-electron repulsion integral within the conventional RI approximation with an auxiliary basis set $\{P\}$. The 3-centered 2-particle density matrix (3C-2PDM) is defined as

$$\begin{aligned} \Pi_{ai}^P = & \Lambda_{ai}^P + \frac{1}{2}\Omega_{ai}^P + \frac{1}{2}X_{ai}^P \\ = & \sum_t \rho_t \left(\bar{\Lambda}_{ai}^P + \frac{1}{2}\bar{\Omega}_{ai}^P \right) + \frac{1}{2}X_{ai}^P \quad (19) \end{aligned}$$

With the intermediate 2PDMs given as

$$\bar{\Lambda}_{ai}^P = \frac{1}{2}(P|R)^{-1/2}(\bar{U}_{RQ}^{-\beta}\bar{S}_{RQ}^{\beta} + \bar{U}_{QR}^{-\beta}\bar{S}_{QR}^{\beta})\bar{B}_{ai}^Q \quad (20)$$

$$\bar{\Omega}_{ai}^P = \beta\bar{x}_{PQ}(\bar{W}_{ai}^Q - \bar{Q}_{ai}^Q) - (P|Q)^{-1/2}\bar{h}_i^Q\bar{b}_i^a - (P|Q)^{-1/2}\bar{h}_i^Q\bar{f}_i^Q \quad (21)$$

$$\begin{aligned} X_{ai}^P = & -P_{ab}\Gamma_{bi}^P + \Gamma_{aj}^P P_{ij} - b_i^a(g^P + \beta g^P) - \\ & (P|R)^{-1/2}(\alpha f^R + \beta f^R)H_{ai} + b_k^a C_{ck}^P H_{ci} + b_i^c C_{ck}^P H_{ak} \quad (22) \end{aligned}$$

Here, Γ is the SOS-MP2 ground-state 2PDM, which can be obtained with³⁶

$$\Gamma_{ai}^P = -\sum_t \rho_t^\beta \tilde{x}_{PQ} \tilde{B}_{ai}^Q \quad (23)$$

The 1-particle density matrix (1PDM) corrections can be derived as

$$P_{ab}^\Pi = -\sum_t \rho_t \tilde{h}_t^a (\tilde{\Lambda}_{bj}^Q + \tilde{\Omega}_{bj}^Q) (aj|Q) \quad (24)$$

$$P_{ij}^\Pi = \sum_t \rho_t \tilde{h}_t^j (\tilde{\Lambda}_{bj}^Q + \tilde{\Omega}_{bj}^Q) (ib|Q) \quad (25)$$

In arriving at these equations, we have used

$$\tilde{h}_t^b t^\beta \tilde{U}_{PQ} - \beta \tilde{S}_{PQ} \tilde{B}_{aj}^P B_{bj}^Q = \tilde{h}_t^a t^\beta \tilde{U}_{QP} - \beta \tilde{S}_{QP} \tilde{B}_{bj}^P B_{aj}^Q \quad (\text{no sum in } a, b) \quad (26a)$$

$$\tilde{h}_t^j t^\beta \tilde{U}_{PQ} - \beta \tilde{S}_{PQ} \tilde{B}_{aj}^P B_{ai}^Q = \tilde{h}_t^i t^\beta \tilde{U}_{QP} - \beta \tilde{S}_{QP} \tilde{B}_{ai}^P B_{aj}^Q \quad (\text{no sum in } i, j) \quad (26b)$$

together with the index symmetries of $\varepsilon_{ab}^{(x)}$ and $\varepsilon_{ij}^{(x)}$.

The energy weighted density matrices (**W**) and the Lagrangian (**L**) can be obtained in a manner similar to the SOS-MP2 or RI-MP2 gradients by defining two intermediate matrices

$$L_{\mu\nu}^{\Pi,1} = \Pi_{aj}^Q (\mu j|Q) \quad (27)$$

$$L_{\nu i}^{\Pi,2} = \Pi_{aj}^Q (a \nu|Q) \quad (28)$$

with the usual designation of μ, ν, \dots for the atomic orbitals. With these definitions, the working expressions of **W** and **L** follow as

$$W_{\mu\nu}^\Pi = -L_{\mu\nu}^{\Pi,1} C_{\mu\nu} \quad (29)$$

$$W_{ij}^\Pi = -L_{vi}^{\Pi,2} C_{vj} \quad (30)$$

$$L_{ai}^\Pi = -L_{\mu i}^{\Pi,1} C_{\mu i} + L_{vi}^{\Pi,2} C_{va} \quad (31)$$

The quantities in the β -space are defined analogously and will not be elaborated here. Finally, the 2-centered 2-particle density matrix (2C-2PDM) is obtained as

$$\begin{aligned} \gamma_{RS}^\Pi = & \sum_t \rho_t [2^\beta \tilde{e}_{RQ}^\alpha \tilde{x}_{SQ} + 2^\beta \tilde{e}_{RQ}^\beta \tilde{x}_{SQ} - \\ & (S|T)^{-1/2} \alpha \tilde{h}^T \tilde{f}^Q (Q|R)^{-1/2} - (S|T)^{-1/2} \beta \tilde{h}^T \alpha \tilde{f}^Q (Q|R)^{-1/2} - \\ & (\alpha g^S + \beta g^S)(\alpha f^Q + \beta f^Q)(Q|R)^{-1/2} + \\ & H_{bk} C_{bj}^R C_{ck}^S b_j^c + H_{bk}^- C_{bj}^R C_{ck}^S b_j^c] \quad (32) \end{aligned}$$

B. Gradient from ω_U Term. Making use of the Laplace transform (eq 9), ω_U can be expressed as

$$\omega_U = -\sum_t \rho_t \mu_{ij}^{\bar{a}b} \exp(-\Delta_{ij}^{\bar{a}b} t) u_{ij}^{\bar{a}b} \quad (33)$$

$$u_{ij}^{\bar{a}b} = (\bar{a}\bar{c}|bj)b_i^{\bar{c}} + (\bar{a}\bar{i}|bc)b_j^{\bar{c}} - (\bar{k}\bar{i}|bj)b_k^{\bar{a}} - (kj|\bar{a}\bar{i})b_k^b \quad (34)$$

and with the help of eq 12, its derivative can be easily formulated as

$$\begin{aligned} [\omega_U]^{(x)} = & -\sum_t 2\rho_t \mu_{ij}^{\bar{a}b} \exp(-\Delta_{ij}^{\bar{a}b} t) [(\bar{a}\bar{c}|bj)^{(x)} b_i^{\bar{c}} + \\ & (\bar{a}\bar{i}|bc)^{(x)} b_j^{\bar{c}} - (\bar{k}\bar{i}|bj)^{(x)} b_k^{\bar{a}} - (kj|\bar{a}\bar{i})^{(x)} b_k^b] - \\ & \sum_t \rho_t \mu_{ij}^{\bar{a}b} \exp(-\Delta_{ij}^{\bar{a}b} t) [-\varepsilon_{\bar{a}\bar{d}}^{(x)} \tilde{h}_{\bar{a}t}^{\bar{d}} u_{ij}^{\bar{a}b} - \varepsilon_{bd}^{(x)} \tilde{h}_{bt}^{\bar{d}} u_{ij}^{\bar{a}b} + \\ & \varepsilon_{i\bar{i}}^{(x)} \tilde{h}_{i\bar{i}}^{\bar{a}} u_{ij}^{\bar{a}b} + \varepsilon_{j\bar{j}}^{(x)} \tilde{h}_{j\bar{j}}^b u_{ij}^{\bar{a}b}] \quad (35) \end{aligned}$$

Similar to $[\omega_T]^{(x)}$, this can be straightforwardly transformed into a compact form after some algebra

$$\begin{aligned} [\omega_U]^{(x)} = & 2M_{aj}^P b_j^b (ab|P)^x + 2M_{\bar{a}j}^P \bar{b}_j^{\bar{a}} (\bar{a}\bar{b}|P)^x - \\ & 2M_{bj}^P b_i^b (ij|P)^x - 2M_{\bar{b}j}^P \bar{b}_i^{\bar{b}} (\bar{i}\bar{j}|P)^x + 2N_{ai}^P (ai|P)^x + \\ & 2N_{\bar{a}i}^P (\bar{a}\bar{i}|P)^x - \gamma_{RS}^D (R|S)^x + W_{ab}^D S_{ab}^x + W_{\bar{a}\bar{b}}^D S_{\bar{a}\bar{b}}^x + \\ & 2W_{ai}^D S_{ai}^x + 2W_{\bar{a}\bar{i}}^D S_{\bar{a}\bar{i}}^x + W_{ij}^D S_{ij}^x + W_{\bar{i}\bar{j}}^D S_{\bar{i}\bar{j}}^x + 2L_{ai}^D U_{ai}^x + \\ & 2L_{\bar{a}\bar{i}}^D U_{\bar{a}\bar{i}}^x + P_{ab}^D \varepsilon_{ab}^{(x)} + P_{\bar{a}\bar{b}}^D \varepsilon_{\bar{a}\bar{b}}^{(x)} + P_{ij}^D \varepsilon_{ij}^{(x)} + P_{\bar{i}\bar{j}}^D \varepsilon_{\bar{i}\bar{j}}^{(x)} \quad (36) \end{aligned}$$

It is easy to show that 3C-2PDMs on each quadrature point are obtained as

$$\tilde{M}_{ai}^P = -\beta \tilde{x}_{PQ} \tilde{D}_{ai}^Q - \beta \tilde{y}_{PQ} \tilde{B}_{ai}^Q \quad (37)$$

$$\tilde{N}_{ai}^P = -\beta \tilde{w}_{PQ} \tilde{D}_{ai}^Q - \beta \tilde{z}_{PQ} \tilde{B}_{ai}^Q \quad (38)$$

with their obvious counterparts in the β -space. The working expression for the 2C-2PDM is

$$\begin{aligned} \gamma_{RS}^D = & -2 \sum_t \rho_t [\beta \tilde{z}_{RQ}^\alpha \tilde{x}_{SQ} + \beta \tilde{y}_{RQ}^\alpha \tilde{w}_{SQ} + \beta \tilde{x}_{RQ}^\alpha \tilde{z}_{SQ} + \\ & \beta \tilde{w}_{RQ}^\alpha \tilde{y}_{SQ}] \quad (39) \end{aligned}$$

and the 1PDM corrections are

$$P_{ab}^D = -\sum_t \rho_t \tilde{h}_t^a t (\tilde{M}_{bj}^Q A_{aj}^Q + \tilde{N}_{bj}^Q (aj|Q)) \quad (40)$$

$$P_{ij}^D = \sum_t \rho_t \tilde{h}_t^j t (\tilde{M}_{bi}^Q A_{bi}^Q + \tilde{N}_{bi}^Q (ib|Q)) \quad (41)$$

also with their obvious counterparts in the β -space. If we define the following two matrices

$$L_{\mu\nu}^{D,1} = N_{aj}^Q (\mu j|Q) + M_{bj}^Q b_j^c (c\mu|Q) + M_{bj}^Q b_j^a (b\mu|Q) \quad (42)$$

$$L_{\nu i}^{D,2} = N_{bi}^Q (b\nu|Q) - M_{bj}^Q b_i^b (\nu j|Q) - M_{bi}^Q b_j^b (\nu j|Q) \quad (43)$$

the energy-weight densities and the Lagrangian, **L**^D and **W**^D, can be obtained analogously to eqs 29–31.

C. Efficient Usage of 3C-2PDMs. For an efficient evaluation of the intermediate **L** and 3-centered force (3CF) terms with $(pqlR)^x$, it is customary to use both the primitive and the back-transformed 3C-2PDMs

$$L_{\mu\nu}^1 = \Gamma_{aj}^Q [(\mu\nu|Q) C_{vj}] \quad (44)$$

$$L_{\nu i}^2 = \Gamma_{\mu i}^Q (\mu\nu|Q) = [\Gamma_{ai}^Q C_{\mu a}] (\mu\nu|Q) \quad (45)$$

$$\Gamma_{ai}^Q (ai|Q)^x = \Gamma_{\mu i}^Q (\mu\nu|Q)^x C_{vi} = [\Gamma_{ai}^Q C_{\mu a}] (\mu\nu|Q)^x C_{vi} \quad (46)$$

Here, the square brackets explicitly show the necessary

Table 1. Definitions of Various Intermediates for Evaluating SOS-CIS(D₀) Gradient^{a-c}

| Laplace quadrature independent | Laplace quadrature dependent |
|--|--|
| $P_{ij} = -b_i^a b_j^a$ | $\tilde{B}_{ai}^P = B_{ai}^P e^{-\varepsilon_a t} e^{\varepsilon_i t}$ |
| $P_{ab} = b_i^a b_i^b$ | $\tilde{D}_{ai}^P = D_{ai}^P e^{-\varepsilon_a t} e^{\varepsilon_i t}$ |
| $B_{aj}^P = (aj R)(R P)^{-1/2}$ | $\tilde{W}_{ai}^P = W_{ai}^P e^{-\varepsilon_a t} e^{\varepsilon_i t}$ |
| $C_{aj}^P = (aj R)(R P)^{-1}$ | $\tilde{Q}_{ai}^P = Q_{ai}^P e^{-\varepsilon_a t} e^{\varepsilon_i t}$ |
| $D_{ai}^P = B_{ab}^P b_i^b - B_{ji}^P b_j^a$ | $\tilde{f}^P = b_i^a \tilde{B}_{ai}^P \tilde{f}^P = \tilde{f}^R (P R)^{-1/2}$ |
| $A_{ai}^P = D_{ai}^R (R P)^{-1/2}$ | $\tilde{I}_{ai} = I_{ai} e^{-\varepsilon_a t} e^{\varepsilon_i t}$ |
| $V_{ij}^P = b_j^a B_{ai}^R$ | $\tilde{X}_{PQ} = B_{ai}^P \tilde{B}_{ai}^Q \tilde{x}_{PQ} = (P R)^{-1/2} \tilde{X}_{RQ}$ |
| $W_{aj}^P = P_{ab} B_{bj}^P$ | $\tilde{Y}_{PQ} = \tilde{D}_{ai}^P B_{ai}^Q = D_{ai}^P \tilde{B}_{ai}^Q$ |
| $Q_{ai}^P = B_{aj}^P P_{ji}$ | $\tilde{Z}_{PQ} = D_{ai}^P \tilde{D}_{ai}^Q \tilde{z}_{PQ} = (P R)^{-1/2} \tilde{Z}_{QR}$ |
| $f^P = b_i^a B_{ai}^P$ | $\tilde{U}_{PQ} = W_{ai}^P \tilde{B}_{ai}^Q = \tilde{W}_{ai}^P B_{ai}^Q$ |
| $J_{ai} = (\alpha f^P + \beta f^P) B_{ai}^P$ | $\tilde{S}_{PQ} = Q_{ai}^P \tilde{B}_{ai}^Q = \tilde{Q}_{ai}^P B_{ai}^Q$ |
| $K_{ai} = B_{aj}^P b_j^b B_{bi}^P$ | $\tilde{Y}_{PQ} = (P R)^{-1/2} \tilde{Y}_{QR}$ |
| $I_{ai} = J_{ai} - K_{ai}$ | $\tilde{W}_{PQ} = (P R)^{-1/2} \tilde{Y}_{RQ}$ |
| $H_{ai} = \sum_t \rho_t^\beta \tilde{x}_{tj}^P \tilde{B}_{ai}^P$ | $\tilde{e}_{PQ} = 1/2 (P R)^{-1/2} (\tilde{U}_{RQ} + \tilde{U}_{QR} - \tilde{S}_{RQ} - \tilde{S}_{QR})$ |
| $g^P = \sum_t \rho_t^\beta \tilde{x}_{PQ}^a \tilde{f}^Q = H_{ai} C_{ai}^P$ | $\tilde{h}^P = \tilde{I}_{bj} B_{bj}^P = I_{bj} \tilde{B}_{bj}^P \tilde{h}^P = \tilde{h}^R (P R)^{-1/2}$ |

^a Only the terms in the α -space are presented. ^b Unless ambiguous, spin designations are omitted for simplicity. ^c Repeated indices implicitly mean summations except with energy weightings, $e^{\pm \varepsilon_p t}$.

contractions. This way, any computation or storage of matrices with the size $\sim VNX$ can be avoided, leaving only much smaller quantities with size $\sim ONX$. (Note that O represents the number of occupied orbitals; V , no. of virtual orbitals; N , no. of basis functions; X , no. of auxiliary basis functions.)

In SOS-CIS(D₀) gradient, the terms involving $\mathbf{\Pi}$ and \mathbf{N} can be trivially evaluated in the same manner. For efficiency, the sum of these two 2PDMs can be used to

invoke these \mathbf{L} and 3CF evaluations. The second and third terms of eq 43 can actually be evaluated together with $\mathbf{\Pi}$ and \mathbf{N} by defining

$$\mathbf{M}_{\mu i}^Q = \mathbf{M}_{bj}^Q b_i^b C_{\mu j} + \mathbf{M}_{bi}^Q b_j^b C_{\mu j} \quad (47)$$

and

$$L_{\mu\mu}^{L,1} = (c_T \mathbf{\Pi}_{aj}^Q + c_U \mathbf{N}_{aj}^Q) [(\mu\nu|Q) C_{\nu j}] \quad (48)$$

$$L_{vi}^{1,2} = (c_T \Pi_{\mu i}^Q + c_U N_{\mu i}^Q - c_U M_{\mu i}^Q)(\mu\nu|Q) \quad (49)$$

Here, c_T and c_U refer to the spin component scaling parameters presented in eq 1. Using $\mu\nu$ index exchange symmetry in $(\mu\nu|Q)^x$, it can be shown that the 3CF terms involving $(ai|Q)^x$ and $(ij|Q)^x$ can also be obtained with

$$(3CF)_I^x = (2c_T \Pi_{\mu i}^Q + 2c_U N_{\mu i}^Q - c_U M_{\mu i}^Q)(\mu\nu|Q)^x C_{vi} \quad (50)$$

It is interesting to note that the same approach can be employed to efficiently evaluate the remaining \mathbf{L} and 3CF terms. For this purpose, we need to define a dressed coefficient

$$D_{vj} = C_{vb} b_j^b \quad (51)$$

and generate the following intermediate \mathbf{L} matrices

$$L_{a\mu}^{II,1} = c_U M_{aj}^Q (\mu\nu|Q) D_{vj} \quad (52)$$

$$L_{vi}^{II,2} = c_U M_{\mu i}^Q (\mu\nu|Q) = c_U [M_{ai}^Q C_{\mu a}] (\mu\nu|Q) \quad (53)$$

Likewise, it is easy to show that the 3CF terms involving $(ab|Q)^x$ is given as

$$(3CF)_{II}^x = 2c_U M_{\mu i}^Q (\mu\nu|Q)^x D_{vi} \quad (54)$$

Then, the final \mathbf{L} matrices from both $[\omega_T]^{(x)}$ and $[\omega_U]^{(x)}$ can be constructed as

$$L_{a\mu}^1 = L_{a\mu}^{I,1} + L_{a\mu}^{II,1} + L_{\mu i}^{II,2} b_i^a \quad (55)$$

$$L_{vi}^2 = L_{vi}^{I,2} \quad (56)$$

Of course, the final 3CF will be the sum of the two contributions, $(3CF)_I$ and $(3CF)_{II}$.

D. Finalizing the Gradient. Up to this point, we have seen how 2PDMs and Lagrangians are built together with the unrelaxed 1PDMs. After obtaining these, the gradient can be calculated in the same manner as in many other

quantum chemical methods.^{14,44,46,51,52} First, to compute the relaxed 1PDM, the \mathbf{Z} -vector equation⁵³ is solved such that

$$\mathbf{AZ} = \mathbf{L} \quad (57)$$

is satisfied together with the usual orbital Hessian \mathbf{A} .^{54,55} Even though the ground- and the excited-state contributions to 1PDM can be calculated separately along with two separate \mathbf{Z} -vectors as their individual relaxations in theory, it is practically more desirable to compute the overall 1PDM and its relaxation by using the combined Lagrangian.

After this, the final construction of the gradient can be performed using the well-known expression

$$E_{\text{SOS-CIS(D}_0\text{)}}^{(x)} = P_{\mu\nu}^{\text{tot}} H_{\mu\nu}^x + W_{\mu\nu}^{\text{tot}} S_{\mu\nu}^x + 2\Gamma_{\mu\nu}^{\text{tot};P} (\mu\nu|P)^x - \gamma_{RS}^{\text{tot}} (R|S)^x + \Gamma_{\mu\nu\lambda\sigma} (\mu\nu|\lambda\sigma)^x \quad (58)$$

Here, we have used “tot” to denote that the density matrices should include contributions from all relevant energy terms (HF, SOS-MP2, and ω) with appropriate scaling parameters. As the explicit expressions of the terms from ω have been described in this section, and as the terms from other contributions are already well-known,^{36,46,56} reiterating the formulation of these terms will be only laborious. Thus, we will leave the details up to the readers. Finally, $\Gamma_{\mu\nu\lambda\sigma}$ represents the separable 2PDM given as

$$\Gamma_{\mu\nu\lambda\sigma} = \left(\frac{1}{2} P_{\mu\nu}^{\text{HF}} + P_{\mu\nu}^{\text{corr}} \right) P_{\lambda\sigma}^{\text{HF}} - \left(\frac{1}{2} P_{\mu\sigma}^{\text{HF}} + P_{\mu\sigma}^{\text{corr}} \right) P_{\lambda\nu}^{\text{HF}} + T_{\mu\nu} T_{\lambda\sigma} - T_{\mu\sigma} T_{\lambda\nu} \quad (59)$$

with HF 1PDM $P_{\mu\nu}^{\text{HF}}$, post-HF density correction $P_{\mu\nu}^{\text{corr}}$, and CIS dressed density-like matrix $T_{\mu\nu}$ defined as⁴⁶

$$T_{\mu\nu} = C_{\mu i} b_i^a C_{va} \quad (60)$$

E. Avoiding Potential Divergence of Exponentials. The factor \tilde{h}_p^q given in eq 16 contains exponential functions with 1-electron orbital energies as their arguments. This may lead

Chart 1. Algorithm of Laplace Loop I and Its CPU and IO Costs

| | | Disk IO cost | CPU cost |
|----|---|--------------|--------------------|
| | Loop over t ($t \in$ quadrature points, size: T) | | |
| | Loop over i ($i \in$ OCC) | | |
| 1 | Read $B_{ai}^p, D_{ai}^p, E_{ai}^p = W_{ai}^p - Q_{ai}^p$ | 3OVXT | |
| 2 | $\tilde{B}_{ai}^p = B_{ai}^p e^{-(e_a - e_i)t}, \tilde{D}_{ai}^p = D_{ai}^p e^{-(e_a - e_i)t}$ | | |
| 3 | $\tilde{f}^p += \sum_a b_i^a \tilde{B}_{ai}^p$ | | |
| 4 | $\tilde{h}^p += \sum_a I_{ai} \tilde{B}_{ai}^p$ | | |
| 5 | $\tilde{X}_{pQ} += \sum_a B_{ai}^p \tilde{B}_{ai}^Q$ | | OVX ² T |
| 6 | $\tilde{Y}_{pQ} += \sum_a D_{ai}^p \tilde{B}_{ai}^Q$ | | OVX ² T |
| 7 | $\tilde{Z}_{pQ} += \sum_a D_{ai}^p \tilde{D}_{ai}^Q$ | | OVX ² T |
| 8 | $(\tilde{U}_{pQ} - \tilde{S}_{pQ}) += \sum_a E_{ai}^p \tilde{B}_{ai}^Q$ | | OVX ² T |
| 9 | Make $\tilde{x}_{pQ}, \tilde{y}_{pQ}, \tilde{w}_{pQ}, \tilde{z}_{pQ}, \tilde{e}_{pQ}, \tilde{f}^p, \tilde{h}^p$ | | |
| 10 | Write $\tilde{x}_{pQ}, \tilde{y}_{pQ}, \tilde{w}_{pQ}, \tilde{z}_{pQ}, \tilde{e}_{pQ}$ | | |
| 11 | $g^p += \sum_i \rho_i \tilde{x}_{pQ} \tilde{f}^Q$ | | |
| 12 | $\gamma_{RS} = c_T \rho_t \sum_Q \tilde{x}_{RQ} \tilde{x}_{SQ}$ | | |
| 13 | $\gamma_{RS}^I += c_T \rho_t \sum_Q (\tilde{e}_{RQ} \tilde{x}_{SQ} + \tilde{x}_{RQ} \tilde{e}_{SQ}) - \tilde{h}^R \tilde{f}^S$ | | |
| 14 | $\gamma_{RS}^D = c_U \rho_t \sum_Q (\tilde{z}_{RQ} \tilde{x}_{SQ} + \tilde{x}_{RQ} \tilde{z}_{SQ} + \tilde{y}_{RQ} \tilde{w}_{SQ} + \tilde{w}_{RQ} \tilde{y}_{SQ})$ | | |

to an ill-behavedness of this factor, especially for low-energy core orbitals and high-energy virtuals and will seriously affect the evaluations of 1PDMs if we directly follow eqs 24, 25, 40, and 41. Thus, the 1PDM equations need to be modified to prevent this potential problem.

We can always avoid this issue if we only use $e^{-\varepsilon_{at}}$ and $e^{\varepsilon_{it}}$ in the working expressions, as the virtual and occupied energies tend to be positive and negative, respectively. Occasional sign switches will not pose any difficulties, as absolute values of such orbital energies will be rather small. Thus, by defining $\bar{\Lambda}_{bj}^Q$ as

$$\bar{\Lambda}_{ai}^P = \tilde{\Lambda}_{ai}^P e^{\varepsilon_{at}} e^{-\varepsilon_{it}} = \beta \tilde{\varepsilon}_{PQ} B_{ai}^Q \quad (61)$$

and by defining $\bar{\Omega}_{ai}^P$, \bar{M}_{ai}^P , and \bar{N}_{ai}^P analogously, we can rewrite the 1PDM expressions as follows

$$P_{ab}^{\Pi} = - \sum_t \rho_t \frac{e^{-\varepsilon_{bt}} - e^{-\varepsilon_{at}}}{\Delta_b^a} (\bar{\Lambda}_{bj}^Q + \bar{\Omega}_{bj}^Q)(aj|Q) e^{\varepsilon_{jt}} \quad (62)$$

$$P_{ij}^{\Pi} = \sum_t \rho_t \frac{e^{\varepsilon_{jt}} - e^{\varepsilon_{it}}}{\Delta_i^j} (\bar{\Lambda}_{bj}^Q + \bar{\Omega}_{bj}^Q)(ib|Q) e^{-\varepsilon_{bt}} \quad (63)$$

$$P_{ab}^D = - \sum_t \rho_t \frac{e^{-\varepsilon_{bt}} - e^{-\varepsilon_{at}}}{\Delta_b^a} (\bar{M}_{bj}^Q A_{aj}^Q + \bar{N}_{bj}^Q (aj|Q)) e^{\varepsilon_{jt}} \quad (64)$$

$$P_{ij}^D = \sum_t \rho_t \frac{e^{\varepsilon_{jt}} - e^{\varepsilon_{it}}}{\Delta_i^j} (\bar{M}_{bj}^Q A_{bi}^Q + \bar{N}_{bj}^Q (ib|Q)) e^{-\varepsilon_{bt}} \quad (65)$$

As is proven in the Appendix, these equations are still valid even with degenerate orbitals when the function $f(p, q) = (e^{pt} - e^{qt})/(p - q)$ is analytically continued toward its singular point ($p = q$). Practically, the following expansion should be adopted to preserve enough numerical precisions in near-degenerate cases

$$\frac{e^{pt} - e^{qt}}{p - q} = te^{(p+q)t/2} \left(1 + \frac{1}{2^2 \cdot 3!} \delta^2 t^2 + \frac{1}{2^4 \cdot 5!} \delta^4 t^4 + \dots \right) \quad (66)$$

with $\delta = p - q$. We have exclusively used these 1PDM

Chart 2. Algorithm of Laplace Loop II (Path 1) and Its CPU and IO Costs

| | Disk IO cost | CPU cost |
|--|---------------|----------------------------------|
| Loop over t ($t \in$ quadrature points, size: T) | | |
| 1 Read $\tilde{x}_{PQ}, \tilde{y}_{PQ}, \tilde{w}_{PQ}, \tilde{z}_{PQ}, \tilde{\varepsilon}_{PQ}$ | | |
| Loop over i ($i \in$ OCC) | | |
| 2 Read $B_{ai}^P, D_{ai}^P, E_{ai}^P = W_{ai}^P - Q_{ai}^P$ | 3OVXT | |
| 3 $H_{ai} \leftarrow \rho_i \sum_P B_{ai}^P e^{-(\varepsilon_i - \varepsilon_P)} \tilde{f}^P$ | | |
| 4 $\bar{\Gamma}_{ai}^P = -\tilde{x}_{PQ} B_{ai}^Q$ | | OVX ² T |
| 5 $\bar{\Omega}_{ai}^P = \tilde{x}_{PQ} E_{ai}^Q - b_{ai}^P \tilde{h}^P - I_{ai} \tilde{f}^P$ | | OVX ² T |
| 6 $\bar{\Lambda}_{ai}^P + r \bar{N}_{ai}^P = (\tilde{\varepsilon}_{PQ} - r \tilde{z}_{PQ}) B_{ai}^Q - r \tilde{w}_{PQ} D_{ai}^Q$ | | 2OVX ² T |
| 7 $r \bar{M}_{ai}^P = -r (\tilde{x}_{PQ} D_{ai}^Q + \tilde{y}_{PQ} B_{ai}^Q)$ | | 2OVX ² T |
| 8 Save $\bar{\Gamma}_{ai}^P$ | OVXT | |
| 9 Save $\bar{\omega}_{ai}^P = \bar{\Gamma}_{ai}^P + \bar{\Omega}_{ai}^P + \bar{\Lambda}_{ai}^P + r \bar{N}_{ai}^P$ | OVXT | |
| 10 Save $\bar{\lambda}_{ai}^P = \bar{\Omega}_{ai}^P / 2 + \bar{\Lambda}_{ai}^P + r \bar{N}_{ai}^P$ | OVXT | |
| 11 Save $\bar{\mu}_{ai}^P = r \bar{M}_{ai}^P$ | OVXT | |
| Loop over i -batch ($i \in$ OCC) | | |
| 12 If ($t > 0$), read $\Gamma_{ai}^P, \lambda_{ai}^P, \mu_{ai}^P$ | 3OVX($T-1$) | |
| 13 Read $\bar{\Gamma}_{ai}^P, \bar{\lambda}_{ai}^P, \bar{\mu}_{ai}^P$ | 3OVXT | |
| 14 $\Gamma_{ai}^P \leftarrow c_i \rho_i \bar{\Gamma}_{ai}^P e^{-\varepsilon_{it}} e^{\varepsilon_{at}}$ | | |
| 15 $\lambda_{ai}^P \leftarrow c_i \rho_i \bar{\lambda}_{ai}^P e^{-\varepsilon_{it}} e^{\varepsilon_{at}}$ | | |
| 16 $\mu_{ai}^P \leftarrow c_i \rho_i \bar{\mu}_{ai}^P e^{-\varepsilon_{it}} e^{\varepsilon_{at}}$ | | |
| 17 Write $\Gamma_{ai}^P, \lambda_{ai}^P, \mu_{ai}^P$ | 3OVXT | |
| 18 Transpose $\bar{\omega}_{ai}^P, \bar{\mu}_{ai}^P$ on disk: $(a, i, P) \leftarrow (a, P, i)$ | 4OVXT | |
| Loop over P ($P \in$ AUX) | | |
| 19 Read $\bar{\omega}_{ai}^P, \bar{\mu}_{ai}^P$ | 2OVXT | |
| 20 Read $(a, i P), A_{ai}^P$ | 2OVXT | |
| 21 $\tilde{P}_{ab} \leftarrow \sum_i \bar{\omega}_{ai}^P (bi P) e^{\varepsilon_{it}}$ | | OV ² X ² T |
| 22 $\tilde{P}_{ij} \leftarrow \sum_a \bar{\omega}_{ai}^P (aj P) e^{-\varepsilon_{at}}$ | | O ² VXT |
| 23 $\tilde{P}_{ab} \leftarrow \sum_i \bar{\mu}_{ai}^P A_{bi}^P e^{\varepsilon_{it}}$ | | OV ² X ² T |
| 24 $\tilde{P}_{ij} \leftarrow \sum_a \bar{\mu}_{ai}^P A_{aj}^P e^{-\varepsilon_{at}}$ | | O ² VXT |
| 25 $P_{ab}^{\text{corr}} \leftarrow c_T \rho_t \tilde{P}_{ab} (e^{-\varepsilon_{bt}} - e^{-\varepsilon_{at}}) / \Delta_b^a$ | | |
| 26 $P_{ij}^{\text{corr}} \leftarrow c_T \rho_t \tilde{P}_{ij} (e^{\varepsilon_{jt}} - e^{\varepsilon_{it}}) / \Delta_i^j$ | | |
| 27 $P_{ab}^{\text{corr}} \leftarrow P_{ab}^{\text{corr}} + P_{ab}$ | | |
| 28 $P_{ij}^{\text{corr}} \leftarrow P_{ij}^{\text{corr}} + P_{ij}$ | | |

Chart 3. Algorithm of Laplace Loop II (Path 2) and Its CPU and IO Costs

| | Disk IO cost | CPU cost |
|--|--------------|-----------|
| 1 Read $\tilde{x}_{PQ}, \tilde{y}_{PQ}, \tilde{w}_{PQ}, \tilde{z}_{PQ}, \tilde{e}_{PQ}$ for all quadrature points | | |
| Loop over i ($i \in \text{OCC}$) | | |
| 2 Read $B_{ai}^p, D_{ai}^p, E_{ai}^p = W_{ai}^p - Q_{ai}^p$ | 3OVX | |
| Loop over t ($t \in$ quadrature points, size: T) | | |
| 3 $H_{ai} += \rho_t \sum_p B_{ai}^p e^{-(\epsilon_a - \epsilon_i)t} \tilde{f}^p$ | | |
| 4 $\bar{\Gamma}_{ai}^p = -\tilde{x}_{PQ} B_{ai}^p$ | | OVX^2T |
| 5 $\bar{\Omega}_{ai}^p = \tilde{x}_{PQ} E_{ai}^p - b_i^a \bar{h}^p - I_{ai} \bar{f}^p$ | | OVX^2T |
| 6 $\bar{\Lambda}_{ai}^p + r \bar{\mathbf{N}}_{ai}^p = (\tilde{e}_{PQ} - r \tilde{z}_{PQ}) B_{ai}^p - r \tilde{w}_{PQ} D_{ai}^p$ | | $2OVX^2T$ |
| 7 $\bar{\mathbf{M}}_{ai}^p = -(\tilde{x}_{PQ} D_{ai}^p + \tilde{y}_{PQ} B_{ai}^p)$ | | $2OVX^2T$ |
| 8 $\Gamma_{ai}^p += c_T \rho_t \bar{\Gamma}_{ai}^p e^{-\epsilon_i t}$ | | |
| 9 $\lambda_{ai}^p += c_T \rho_t (\bar{\Omega}_{ai}^p / 2 + \bar{\Lambda}_{ai}^p + r \bar{\mathbf{N}}_{ai}^p) e^{-\epsilon_i t} e^{\epsilon_i t}$ | | |
| 10 $\mu_{ai}^p += c_U \rho_t \bar{\mathbf{M}}_{ai}^p e^{-\epsilon_i t} e^{\epsilon_i t}$ | | |
| 11 Write $\bar{\omega}_{ai}^p(t) = \bar{\Gamma}_{ai}^p + \bar{\Omega}_{ai}^p + \bar{\Lambda}_{ai}^p + r \bar{\mathbf{N}}_{ai}^p$ | $OVXT$ | |
| 12 Write $\bar{\mu}_{ai}^p(t) = r \bar{\mathbf{M}}_{ai}^p$ | $OVXT$ | |
| 13 Write $\Gamma_{ai}^p, \lambda_{ai}^p, \mu_{ai}^p$ | 3OVX | |
| 14 Transpose $\bar{\omega}_{ai}^p, \bar{\mu}_{ai}^p$ on disk: $(a, t, i, P) \leftarrow (a, P, t, i)$ | 4OVXT | |
| Loop over P ($P \in \text{AUX}$) | | |
| 15 Read $(a, i P), A_{ai}^p$ | 2OVX | |
| Loop over t ($t \in$ quadrature points, size: T) | | |
| 16 Read $\bar{\omega}_{ai}^p, \bar{\mu}_{ai}^p$ | 2OVXT | |
| 17 $\tilde{P}_{ab} = \sum_i \bar{\omega}_{ai}^p(bi P) e^{\epsilon_i t} + \sum_i \bar{\mu}_{ai}^p A_{bi}^p e^{\epsilon_i t}$ | | $2OV^2XT$ |
| 18 $\tilde{P}_{ij} = \sum_a \bar{\omega}_{ai}^p(aj P) e^{-\epsilon_a t} + \sum_a \bar{\mu}_{ai}^p A_{aj}^p e^{-\epsilon_a t}$ | | $2O^2VXT$ |
| 19 $P_{ab}^{\text{corr}} = c_T \rho_t \tilde{P}_{ab} (e^{-\epsilon_i t} - e^{-\epsilon_a t}) / \Delta_b^a$ | | |
| 20 $P_{ij}^{\text{corr}} += c_T \rho_t \tilde{P}_{ij} (e^{\epsilon_i t} - e^{\epsilon_j t}) / \Delta_i^j$ | | |
| 21 $P_{ab}^{\text{corr}} \leftarrow P_{ab}^{\text{corr}} + P_{ab}$ | | |
| 22 $P_{ij}^{\text{corr}} \leftarrow P_{ij}^{\text{corr}} + P_{ij}$ | | |

representations in the actual implementation, which will be presented in the next section.

III. Implementation

As one can see in the above section, SOS-CIS(D₀) gradient equation involves numerous intermediate terms. In addition, the excited-state gradient calculation should always include the concurrent evaluation of the ground-state gradient. Therefore, the routines that calculate these various intermediates must be carefully designed to minimize the processor and the disk usage. For this purpose, the gradient is obtained with the following algorithm.

A. Pre-Laplace Quadrature Loop. The purpose of this routine is to build intermediates that will be used in the main Laplace loop detailed in the upcoming subsections. All the quadrature-independent terms listed in Table 1 need to be evaluated here except H_{ai} and g^p . Besides the fact that their formulation is quite straightforward, its computational cost is rather small when it is compared to the cost of the Laplace loop, because this routine is executed only once. In addition, certain terms can be inherited from the result of the iteration for the excitation amplitude **b**. Therefore, we will not elaborate on the detailed performance consideration of this part.

B. Laplace Quadrature Loop I. This part aims to form various Laplace quadrature dependent intermediates and portions of 2C-2PDMs. As this routine involves a significant

amount of fourth-order steps in each pass of the Laplace loop, its efficiency is an important issue for consideration. The detailed scheme is presented in Chart 1, together with its expected processor cost.

C. Laplace Quadrature Loop II: Path 1. This routine performs the main calculations for the various 3C-2PDMs and the 1PDMs that will be later used in the gradient evaluation through integrals. Unlike the ground-state SOS-MP2 analytical gradient case,³⁶ because the forms of 3C-2PDMs adopted in the 3-centered force evaluation (eq 19) and 1PDM generation (eqs 24 and 25) are somewhat different, the various components of 3C-2PDMs need to be stored on disk individually. This will significantly increase the disk IO cost compared to the equivalent portion of the fourth-order scaling ground-state gradient theory.³⁶ In Chart 2, one can see that the 3C-2PDMs are scaled and combined in varying forms ($\bar{\omega}_{ai}^p, \bar{\lambda}_{ais}^p$ and $\bar{\mu}_{ai}^p$). The purpose of using these altered forms of 2PDMs together with an intermediate scaling parameter, $r = c_U/c_T$, is to reduce this IO cost. After this modification, the associated IO cost is only about twice of the ground-state case.

D. Laplace Quadrature Loop II: Path 2. In fact, the IO cost of Path 1 presented above can be further improved when we are willing to pay more cost for memory and disk storages. This can easily be inferred by observing that much of the IO cost in Path 1 is involved with the increment of 2PDMs at different Laplace quadrature points (lines 12–17

Chart 4. Algorithm of Post-Laplace Loop and Its CPU and IO Costs

| | Disk IO cost | CPU cost |
|--|--------------|----------|
| Loop over i ($i \in \text{OCC}$) | | |
| 1 Read $B_{ai}^p, V_{j(i)}^p$ | ONX | |
| 2 $v_{j(i)}^p = \sum_Q V_{j(i)}^Q (Q P)^{-1/2}$ | | O^2X^2 |
| 3 ${}_1X_{ai}^p = \sum_j H_{aj} v_{j(i)}^p$ | | O^2VX |
| 4 Write ${}_1X_{ai}^p$ | OVX | |
| 5 $C_{ai}^p = \sum_Q B_{ai}^Q (Q P)^{-1/2}$ | | OVX^2 |
| 6 $w_{(j)i}^p = \sum_a H_{aj} C_{ai}^p$ | | O^2VX |
| 7 Write $w_{(j)i}^p$ | O^2X | |
| 8 $\gamma_{RS}^\Pi += c_T \sum_j v_{j(i)}^R w_{(j)i}^S$ | | |
| 9 $\gamma_{RS}^\Pi := c_T g^R \sum_p (\alpha f^p + \beta f^p)(P R)^{-1/2}$ | | |
| 10 Increment λ_{ai}^p on disk: $\lambda_{ai}^p \leftarrow \lambda_{ai}^p + c_T \cdot {}_1X_{ai}^p / 2$ | 3OVX | |
| 11 Transpose $w_{(i),j}^p$ on disk: $(P, (i), j) \leftarrow (P, j, (i))$ | $2O^2X$ | |
| Loop over i ($i \in \text{OCC}$) | | |
| 12 Read $w_{j(i)}^p$ | O^2X | |
| 13 ${}_2X_{ai}^p = \sum_j b_j^\alpha w_{j(i)}^p$ | | |
| 14 ${}_2X_{ai}^p := H_{ai} \sum_R (\alpha f^R + \beta f^R)(P R)^{-1/2}$ | | |
| 15 ${}_2X_{ai}^p := b_i^\alpha (\alpha g^p + \beta g^p)$ | | |
| 16 Write ${}_2X_{ai}^p$ | OVX | |
| 17 Increment λ_{ai}^p on disk: $\lambda_{ai}^p \leftarrow \lambda_{ai}^p + c_T \cdot {}_2X_{ai}^p / 2$ | 3OVX | |
| 18 Transpose λ_{ai}^p on disk: $(a, i, P) \leftarrow (a, P, i)$ | $2OVX$ | |
| 19 Transpose Γ_{ai}^p on disk: $(a, i, P) \leftarrow (a, P, i)$ | $2OVX$ | |
| Loop over P ($P \in \text{AUX}$) | | |
| 20 Read $\Gamma_{ai}^p, \lambda_{ai}^p$ | $2OVX$ | |
| 21 ${}_3X_{ai}^p = -\sum_b P_{ab} \Gamma_{bi}^p + \sum_j P_{aj} \Gamma_{aj}^p$ | | $OVNX$ |
| 22 Write $\lambda_{ai}^p \leftarrow \lambda_{ai}^p + \Gamma_{ai}^p + {}_3X_{ai}^p / 2$ | OVX | |

in Chart 2). At the first glance, one might expect that this cost can be significantly reduced if the 2PDMs are kept in the core memory. However, this will require cubic memory storage, which will be unacceptably large for many sizable molecules.

The IO cost reduction can actually be attained by switching the order of Laplace and occupied loops. Namely, when the Laplace loop is executed for one selected occupied orbital, 2PDM increments can be performed within the core memory while keeping the memory requirement to be quadratic. This implementation is shown in Chart 3 along with its associated IO and CPU cost. From Charts 2 and 3, one can deduce that the IO cost reduction from this algorithm is from $24OVXT$ down to $\sim 9OVXT$ (assuming $T = 7^{30,32}$).

There are two drawbacks for adopting this algorithm. These are the necessity for storing two quadrature-dependent densities ($\bar{\omega}_{ai}^p$ and $\bar{\mu}_{ai}^p$) on disk at all quadrature points, and the use of T -times larger memory for storing $\tilde{x}, \tilde{y}, \tilde{z}, \tilde{w}$, and \tilde{e} (line 1 in Chart 3). However, the disk storage is usually abundant in modern computational platforms, and this shortcoming associated with the necessary disk space will be mostly insignificant in any practical calculations. The memory requirement will be similarly insignificant: even for a system with 10,000 auxiliary basis functions, the required space for storing the above five matrices will only be 4 gigabytes. More importantly, the required disk and memory storage can always be calculated before entering the Laplace Loop II, and when the available space becomes an issue,

Path 1 can be followed as a fallback mechanism without any difficulties.

E. Post-Laplace Quadrature Loop for 2PDM. The remaining 2PDM components after completing the Laplace loops are evaluated in this routine. Even though there are various elements computed in this routine as detailed in Chart 4, the associated computational cost is relatively small as this routine does not involve the quadrature points. After completing this routine, all 2PDMs are accumulated and stored on disk for their subsequent use in the evaluation of the force terms through the use of integrals in the atomic orbital basis.⁵⁷

F. Force and Lagrangian Evaluations Using Atomic Orbital Based Integrals. With all the density matrices prepared in the above, we are now ready to compute various force terms using the integrals with atomic orbital basis. This is performed concurrently with the construction of Lagrangians in the mixed representations (eqs 44 and 45) as it uses the same density matrices and their transforms⁴⁴ as shown in Chart 5. Practically, this part contains two calls of one identical subroutine with two different AO to MO transformation coefficients ($C_{\mu i}$ and $D_{\mu i}$) and two different sets of 2PDM matrices (λ_{ai}^p and μ_{ai}^p as defined in Charts 2 and 3). The mathematical background for doing this is explained in the previous section. As the structure of the common subroutine closely resembles the one in RI-MP2 gradient calculation for obtaining \mathbf{L} and 3-centered force,⁴⁴ this part can be easily implemented with minor modifications on any

Chart 5. Algorithm of Force and Lagrangian Evaluations through Atomic Orbital Based Integrals

| | Disk IO cost | CPU cost |
|--|--------------------|--------------|
| Loop over P ($P \in \text{AUX}$) | | |
| 1 Read $\lambda_{ai}^p, \mu_{ai}^p$ | 2OVX | |
| 2 Back-transform: $\lambda_{\mu i}^p = \sum_a C_{\mu a} \lambda_{ai}^p$ | ONX | OVNX |
| 3 Back-transform: $\mu_{\mu i}^p = \sum_{a,j} (C_{\mu j} \mu_{aj}^p b_i^a + C_{\mu j} \mu_{ai}^p b_j^a)$ | ONX | $2O^2(I+N)X$ |
| Loop over P -batch ($P \in \text{AUX}$) | | |
| 4 Read $\lambda_{ai}^p, \lambda_{\mu i}^p, \mu_{\mu i}^p$ | $\sim 3\text{ONX}$ | |
| 5 Make $(\mu\nu P)$ | | |
| 6 $L_{vi}^{l,2} += \sum_{\mu,p} (\lambda_{\mu i}^p - \mu_{\mu i}^p)(\mu\nu P)$ | | ON^2X |
| 7 Transform: $(i\nu P) = \sum_{\mu} C_{\mu i}(\mu\nu P)$ | | ON^2X |
| 8 $L_{av}^{l,1} += \sum_{i,p} \lambda_{ai}^p(i\nu P)$ | | OVNX |
| 9 Make $(\mu\nu P)^x$ | | |
| 10 $E^{(x)} += \sum_{i,\mu,\nu,p} (2\lambda_{\mu i}^p - \mu_{\mu i}^p) C_{vi}(\mu\nu P)^x$ | | $\sim ON^2X$ |
| Loop over P ($P \in \text{AUX}$) | | |
| 11 Read μ_{ai}^p | OVX | |
| 12 Back-transform: $\mu_{\mu i}^p = \sum_a C_{\mu a} \mu_{ai}^p$ | ONX | OVNX |
| Loop over P -batch ($P \in \text{AUX}$) | | |
| 13 Read $\mu_{ai}^p, \mu_{\mu i}^p$ | $\sim 2\text{OVX}$ | |
| 14 Back-transform: $\mu_{\mu i}^p = \sum_a C_{\mu a} \mu_{ai}^p$ | ONX | OVNX |
| 15 Make $(\mu\nu P)$ | | |
| 16 $L_{vi}^{ll,2} += \sum_{\mu,p} \mu_{\mu i}^p(\mu\nu P)$ | | ON^2X |
| 17 Transform: $(i\nu P)' = \sum_{\mu} D_{\mu i}(\mu\nu P)$ | | ON^2X |
| 18 $L_{av}^{ll,1} += \sum_{i,p} \mu_{ai}^p(i\nu P)'$ | | OVNX |
| 19 $E^{(x)} += 2 \sum_{i,\mu,\nu,p} \mu_{\mu i}^p D_{vi}(\mu\nu P)^x$ | | $\sim ON^2X$ |
| 20 $L_{av}^l = L_{av}^{l,1} + L_{av}^{ll,1} + \sum_i L_{vi}^{ll,2} b_i^a, L_{vi}^l = L_{vi}^{l,2}$ | | |
| 21 Make $(P Q)^x$ | | |
| 22 $E^{(x)} -= \sum_{P,Q} \gamma_{PQ}^{\text{total}} (P Q)^x$ | | |

Table 2. CPU Times for Calculating SOS-MP2 Ground-State and SOS-CIS(D₀) Excited-State Gradients^a

| molecule | no. of basis | CPU time (min) | | ratio |
|--|------------------|----------------|--------------------------|-------------|
| | | SOS-MP2 | SOS-CIS(D ₀) | |
| hexatriene (C ₆ H ₈) | 460 ^b | 139 (88) | 181 (119) | 1.30 (1.35) |
| styrene (C ₈ H ₈) | 552 ^b | 341 (202) | 462 (283) | 1.35 (1.40) |
| azulene (C ₁₀ H ₈) | 644 ^b | 691 (347) | 884 (469) | 1.28 (1.35) |
| anthracene (C ₁₄ H ₁₀) | 874 ^b | 1805 (1031) | 2002 (1290) | 1.11 (1.25) |
| pyrene (C ₁₆ H ₁₀) | 966 ^b | 3183 (1851) | 3090 (1988) | 0.97 (1.07) |
| ZnBC-BC (C ₄₆ H ₃₆ N ₈ Zn) ^c | 918 ^d | 576 (450) | 1667 (1510) | 2.90 (3.36) |

^a Measured with a 2.0 GHz Opteron processor. Numbers in parentheses are based on CPU times excluding the load for solving Z-vectors. Timing data exclude the cost for solving the HF-SCF equation and the single excitation amplitude **b**. ^b With aug-cc-pVTZ and its corresponding auxiliary basis sets (refs 58 and 59). ^c Structure given in ref 38. ^d With 6-31G(d) and the VDZ auxiliary basis sets (ref 15).

existing RI-MP2 gradient code. This practical convenience is why there are two separate integration batching loops in Chart 5.

IV. Demonstration and Concluding Remarks

The above analytical SOS-CIS(D₀) gradient algorithm has been implemented in the development version of Q-Chem 3.1,⁵⁷ and its performance was benchmarked with selected molecules with varying sizes. The molecules adopted during this benchmark process are listed in Table 2, together with the measured computational costs. Since we aim our new method to have similar efficiency as its sister ground-state gradient theory SOS-MP2,³⁶ comparing the performances of the two methods will be an important task. Thus, in Table

2, we have presented the timing data from SOS-MP2 gradient calculation as well as the timing for our new SOS-CIS(D₀) gradient. For both methods, as the CPU time has been found to be very close to the wall-clock time in most cases, we will only focus on comparing the CPU time.

From Table 2, we can clearly see that the efficiency of our SOS-CIS(D₀) gradient is very close to that of SOS-MP2 gradient. In fact, a detailed comparison of the algorithm charts presented in the previous section with the ones in ref 36 reveals that the routine for calculating various 3-centered density matrices is $\sim 5\times$ more expensive than the corresponding part in SOS-MP2 theory, while performing 1PDM calculations, AO-based integrals, and their associated matrix transformations is approximately twice more expen-

Table 3. CPU Times for Calculating Analytical Gradients at Various Levels of Theory^a

| molecule | no. of basis | CPU time (min) | | |
|---|------------------|----------------|------|--------------------------|
| | | HF | CIS | SOS-CIS(D ₀) |
| hexatriene (C ₆ H ₈) | 460 ^b | 0.3 | 134 | 181 |
| styrene (C ₈ H ₈) | 552 ^b | 0.5 | 339 | 462 |
| azulene (C ₁₀ H ₈) | 644 ^b | 1 | 730 | 884 |
| anthracene (C ₁₄ H ₁₀) | 874 ^b | 3 | 1629 | 2002 |
| pyrene (C ₁₆ H ₁₀) | 966 ^b | 4 | 2707 | 3090 |
| ZnBC-BC (C ₄₆ H ₃₆ N ₈ Zn) | 918 ^c | 44 | 182 | 1667 |

^a Measured with a 2.0 GHz Opteron processor. Timing data exclude the cost for solving the HF-SCF equation and the single excitation amplitude **b**. ^b With aug-cc-pVTZ and its corresponding auxiliary basis sets (refs 58 and 59). ^c With 6-31G(d) and the VDZ auxiliary basis sets (ref 15).

sive. The common routine for building portions of **L** and **W** by contracting unrelaxed and relaxed IPDM with AO-based ERIs will cost the same. The routine for solving the **Z**-vector equation will also cost similarly, although the actual relative cost will vary depending on the number of iterations required to reach convergences in the ground-state and excited-state cases. The result from Table 2 can be understood on this ground: the relative CPU cost is close to 1.0 when the load for obtaining the **Z**-vector solution is dominant (the case with the aug-cc-pVTZ basis⁵⁸), while it reaches ~ 3.0 as other routines become more important. As explained above, our method will cost $\sim 5\times$ more even in the worst case scenario, and in any practical calculations we expect it to perform close to the efficient SOS-MP2 gradient.³⁶

We can see a similar behavior when we compare the cost for obtaining CIS and SOS-CIS(D₀) gradients as presented in Table 3. Unless the system size becomes large enough as in the case of ZnBC-BC complex, the additional cost for including electron correlation effect (CIS \rightarrow SOS-CIS(D₀)) in the gradient evaluation is effectively insignificant because the cost for executing the common routines mentioned in the above are dominant. Of course, evaluating HF gradient after SCF convergence does not require such routines (for example, HF gradient does not require the **Z**-vector), and its cost is almost negligible as shown in Table 3.

In fact, because the computation of the gradient always require executing pregradient routines for reaching HF-SCF solution and for obtaining **b**-amplitudes as eigensolutions of the response matrices, and because these pregradient routines are relatively expensive due to their iterative nature, the most practical comparison should be made by examining the total CPU costs associated with both pregradient and gradient routines. This comparison is schematically presented in Figure 1 for the selected molecules. Again, from this figure, one can be assured that the efficiency of SOS-CIS(D₀) is comparable to other presented methods in general. The only exception is the ZnBC-BC complex. In this molecule, AO-based HF-SCF and CIS solutions are obtained relatively fast because many function pairs are ignored in the integrals due to the large size the system and the relatively low quality of the adopted basis set.

In summary, we have shown that an analytic gradient of SOS-CIS(D₀) can be obtained with a fourth-order computational effort as in the case of its sister ground-state theory,

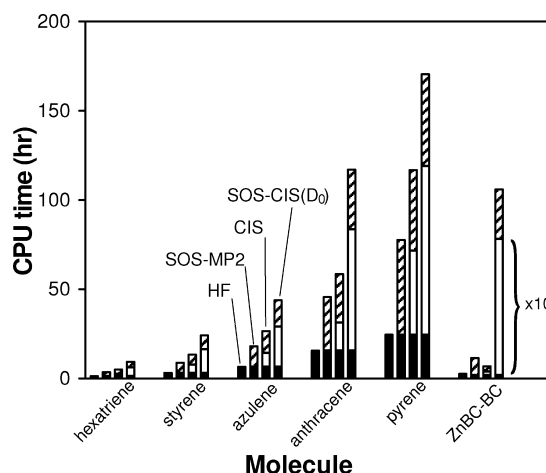


Figure 1. Analysis of total CPU times for obtaining analytical gradients at various levels of theory. Four vertical bars, from left to right, for each molecule represent the total CPU time with HF, SOS-MP2, CIS, and SOS-CIS(D₀) respectively, as denoted in the figure. Different segments of the bars are coded as follows: filled bars (HF-SCF timing), empty bars (CIS or SOS-CIS(D₀) excitation amplitude solution), and hashed bars (gradient calculation). The CPU time for reaching SOS-CIS(D₀) amplitude solution with ZnBC-BC was downscaled by a factor of 10 for visual clarity. A threshold of 10^{-12} au was employed for integral screening, while the convergence criteria for SCF and **b**-amplitude solutions were set to 10^{-7} au and 10^{-6} au, respectively. Other computational details are described in Table 3.

SOS-MP2. This efficiency is attained from the use of Laplace transform in combination with the RI approximation. After implementing this new theory into an efficient algorithm, the actual processor time for calculating the excited-state gradient was found to be comparable to the ground-state gradient calculation time for many molecules. In fact, because the SOS-CIS(D₀) excitation amplitude and energy evaluation involves about 10 additional iteration steps after the conventional SCF solution, the cost for evaluating gradient will be effectively minor. This was indeed true at least for the systems adopted during our benchmark with at most 37% of post SCF calculation time spent on the gradient calculation.

Accordingly, as an efficient wave function-based excited-state gradient theory with a capability of properly describing quasidegenerate states, this method will be useful in studying various quantum chemical systems. Its utility will be diverse ranging from performing a simple excited-state geometry optimization to studying complex dynamics in various photophysical systems. Indeed, we note that various excited-state geometry searches have relied on the electron-uncorrelated CIS gradient, even when the resulting geometries were used for parametrizing an electron-correlated excited theory such as SOS-CIS(D).^{30,32} This was simply due to the previous lack of an efficient wave function-based electron-correlated gradient theory. Thus, applying the present method to such parametrization processes along with numerical comparisons of the various excited-state parameters will be an interesting and important task. We hope to report on this development in due course.

Acknowledgment. This work was supported by a subcontract from Q-Chem Inc, from an NIH SBIR grant, and was also supported by the Office of Basic Energy Sciences of the U.S. Department of Energy through the LBL Ultrafast Center. We are grateful for a grant of supercomputer time from NERSC. D.C. acknowledges financial support from a Fulbright Fellowship. M.H.G. is a part-owner of Q-Chem Inc.

Appendix A: Derivation of $[e^{-\Delta t}]^{(x)}$

From $e^{-\Delta t} = \sum_{n=0}^{\infty} (-)^n \Delta^n t^n / n!$, we can express the derivative as

$$\begin{aligned} [e^{-\Delta t}]^{(x)} &= \sum_{n=1}^{\infty} \sum_{m=0}^{n-1} \frac{1}{n!} (-)^n \Delta^{n-m-1} \Delta^{(x)} \Delta^m t^n \\ &= \sum_{n=0}^{\infty} \sum_{m=0}^n \frac{1}{(n+1)!} (-)^{n+1} \Delta^{n-m} \Delta^{(x)} \Delta^m t^{n+1} \end{aligned} \quad (\text{A1})$$

Note that we can always set Δ as diagonal after SCF completes

$$\Delta_{ijab;i'j'a'b'} = \delta_{ii'} \delta_{aa'} \delta_{jj'} \delta_{bb'} (\epsilon_a + \epsilon_b - \epsilon_i - \epsilon_j) = \Delta_{ij}^{ab} \quad (\text{A2})$$

and $\Delta^{(x)}$ is block-diagonal as

$$\Delta_{ijab;i'j'a'b'}^{(x)} = \delta_{ii'} \epsilon_{aa'}^{(x)} \delta_{jj'} \delta_{bb'} + \delta_{ii'} \delta_{aa'} \delta_{jj'} \epsilon_{bb'}^{(x)} - \epsilon_{ii'}^{(x)} \delta_{aa'} \delta_{jj'} \delta_{bb'} - \delta_{ii'} \delta_{aa'} \epsilon_{jj'}^{(x)} \delta_{bb'} \quad (\text{A3})$$

Because of this diagonal and block-diagonal nature, the matrix multiplications in eq A1 can be performed with relative ease, and its elements can be expressed as

$$\begin{aligned} [e^{-\Delta t}]_{ijab;i'j'a'b'}^{(x)} &= \sum_{n=0}^{\infty} \sum_{m=0}^n \frac{1}{(n+1)!} (-)^{n+1} t^{n+1} (\Delta_{ij}^{ab})^{n-m} \times \\ &\quad [(\Delta_{ij}^{ab})^m \epsilon_{aa'}^{(x)} \delta_{ii'} \delta_{jj'} \delta_{bb'} + (\Delta_{ij}^{ab})^m \delta_{ii'} \delta_{aa'} \delta_{jj'} \epsilon_{bb'}^{(x)} - \\ &\quad (\Delta_{ij}^{ab})^m \epsilon_{ii'}^{(x)} \delta_{aa'} \delta_{jj'} \delta_{bb'} - (\Delta_{ij}^{ab})^m \delta_{ii'} \delta_{aa'} \epsilon_{jj'}^{(x)} \delta_{bb'}] \end{aligned} \quad (\text{A4})$$

Because $\Delta_{ij}^{ab} = \Delta_{ij}^{ab} + \Delta_a^{a'}$ with $\Delta_a^{a'} = \epsilon_{a'} - \epsilon_a$, the first term in eq A4 becomes

$$\begin{aligned} [e^{-\Delta t}]_{ijab;i'j'a'b'}^{(x)} &= \sum_{n=0}^{\infty} \sum_{m=0}^n \frac{1}{(n+1)!} (-)^{n+1} t^{n+1} \times \\ &\quad (\Delta_{ij}^{ab})^{n-m} (\Delta_{ij}^{ab} + \Delta_a^{a'})^m \epsilon_{aa'}^{(x)} \delta_{ii'} \delta_{jj'} \delta_{bb'} \\ &= \sum_{n=0}^{\infty} \sum_{m=0}^n \frac{1}{(n+1)!} (-)^{n+1} t^{n+1} (\Delta_{ij}^{ab})^{n-m} \times \\ &\quad \sum_{r=0}^m C_r (\Delta_a^{a'})^r (\Delta_{ij}^{ab})^{m-r} \epsilon_{aa'}^{(x)} \delta_{ii'} \delta_{jj'} \delta_{bb'} \end{aligned} \quad (\text{A5})$$

with the use of a binomial expansion. Now, we can rearrange the summations to simplify this expression. From the following two relations

$$\sum_{n=0}^{\infty} \sum_{m=0}^n f(m, n) = \sum_{m=0}^{\infty} \sum_{n=0}^{\infty} f(m, n+m) \quad (\text{A6})$$

$$\sum_{m,n=0}^{\infty} f(m, m+n) = \sum_{s=0}^{\infty} \sum_{m=0}^s f(m, s) \quad (\text{A7})$$

we can show that eq A5 can be transformed as

$$\begin{aligned} [e^{-\Delta t}]_{ijab;i'j'a'b'}^{(x)} &= \epsilon_{aa'}^{(x)} \delta_{ii'} \delta_{jj'} \delta_{bb'} \sum_{r=0}^{\infty} \sum_{s=0}^{\infty} \sum_{m=0}^s \frac{1}{(s+r+1)!} (-t)^{s+r+1} \times \\ &\quad (\Delta_{ij}^{ab})^s (\Delta_a^{a'})^r C_m \\ &= \epsilon_{aa'}^{(x)} \delta_{ii'} \delta_{jj'} \delta_{bb'} \sum_{r=0}^{\infty} \sum_{s=0}^{\infty} \frac{1}{(s+r+1)!} (-t)^{s+r+1} \times \\ &\quad (\Delta_{ij}^{ab})^s (\Delta_a^{a'})^r \sum_{m=0}^s C_m \end{aligned} \quad (\text{A8})$$

One can also easily prove that

$$\sum_{m=0}^s C_m = C_{s+1} \quad (\text{A9})$$

is satisfied, and when $\Delta_a^{a'} \neq 0$, eq A8 reduces to the following simple expression

$$[e^{-\Delta t}]_{ijab;i'j'a'b'}^{(x)} = \epsilon_{aa'}^{(x)} \delta_{ii'} \delta_{jj'} \delta_{bb'} e^{-\Delta_{ij}^{ab} t} \frac{1}{\Delta_a^{a'}} [e^{-\Delta_a^{a'} t} - 1] \quad (\text{A10})$$

If $\Delta_a^{a'} = 0$, the binomial expansion in eq A5 leads to

$$[e^{-\Delta t}]_{ijab;i'j'a'b'}^{(x)}|_{\Delta_a^{a'}=0} = -t \epsilon_{aa'}^{(x)} \delta_{ii'} \delta_{jj'} \delta_{bb'} e^{-\Delta_{ij}^{ab} t} \quad (\text{A11})$$

and the analytic continuation of eq A10 to the pole of $\Delta_a^{a'}$ is a valid approach

$$[e^{-\Delta t}]_{ijab;i'j'a'b'}^{(x)}|_{\Delta_a^{a'}=0} = \lim_{\Delta_a^{a'} \rightarrow 0} ([e^{-\Delta t}]_{ijab;i'j'a'b'}^{(x)}) \quad (\text{A12})$$

Namely, eq A10 can be used for any energy eigenvalues. Practically, when the energy difference ($\Delta_a^{a'}$) is smaller than some cutoff value, the Taylor expansion of $(1 - e^{-x})/x = 1 - x/2 + x^2/3! - x^3/4! + \dots$ should be adopted to preserve the numerical precision.

The remaining three terms in eq A4 can be obtained in a similar manner, and the final expression for the matrix derivative is

$$\begin{aligned} [e^{-\Delta t}]_{ijab;i'j'a'b'}^{(x)} &= -t \epsilon_{aa'}^{(x)} \delta_{ii'} \delta_{jj'} \delta_{bb'} e^{-\Delta_{ij}^{ab} t} h(\Delta_a^{a'} t) - \\ &\quad t \epsilon_{bb'}^{(x)} \delta_{ii'} \delta_{jj'} \delta_{aa'} e^{-\Delta_{ij}^{ab} t} h(\Delta_b^{b'} t) + t \epsilon_{ii'}^{(x)} \delta_{jj'} \delta_{aa'} \delta_{bb'} e^{-\Delta_{ij}^{ab} t} h(\Delta_i^{i'} t) + \\ &\quad t \epsilon_{jj'}^{(x)} \delta_{ii'} \delta_{aa'} \delta_{bb'} e^{-\Delta_{ij}^{ab} t} h(\Delta_j^{j'} t) \end{aligned} \quad (\text{A13})$$

with $h(x) = (1 - e^{-x})/x$.

References

- (1) del Bene, J. E.; Ditchfield, R.; Pople, J. A. *J. Chem. Phys.* **1971**, 55, 2236.
- (2) Koch, H.; Jørgensen, P. *J. Chem. Phys.* **1990**, 93, 3333.
- (3) Monkhorst, H. J. *Int. J. Quantum Chem. Symp.* **1977**, 11, 421.
- (4) Mukherjee, D.; Mukherjee, P. *Chem. Phys.* **1979**, 39, 325.

- (5) Emrich, K. *Nucl. Phys. A* **1981**, 351, 392.
- (6) Sekino, H.; Bartlett, R. J. *Int. J. Quantum Chem. Symp.* **1984**, 18, 225.
- (7) Bartlett, R. J. *Modern Electronic Structure Theory*; World Scientific: Singapore, 1995.
- (8) Runge, E.; Gross, E. K. U. *Phys. Rev. Lett.* **1984**, 52, 997.
- (9) Gross, E. K. U.; Kohn, W. *Phys. Rev. Lett.* **1985**, 55, 2850.
- (10) Feyereisen, M.; Fitzgerald, G.; Komornicki, A. *Chem. Phys. Lett.* **1993**, 208, 359.
- (11) Vahtras, O.; Almlöf, J.; Feyereisen, M. W. *Chem. Phys. Lett.* **1993**, 213, 514.
- (12) Hättig, C.; Hald, K. *Phys. Chem. Chem. Phys.* **2002**, 4, 2111.
- (13) Hättig, C.; Weigend, F. *J. Chem. Phys.* **2000**, 113, 5154.
- (14) Weigend, F.; Häser, M. *Theor. Chem. Acc.* **1997**, 97, 331.
- (15) Weigend, F.; Häser, M.; Patzelt, H.; Ahlrichs, R. *Chem. Phys. Lett.* **1998**, 294, 143.
- (16) Werner, H.-J.; Manby, F. R.; Knowles, P. J. *J. Chem. Phys.* **2003**, 118, 8149.
- (17) Whitten, J. L. *J. Chem. Phys.* **1973**, 58, 4496.
- (18) Dunlap, B. I.; Connolly, J. W. D.; Sabin, J. R. *J. Chem. Phys.* **1979**, 71, 3396.
- (19) Almlöf, J. *Chem. Phys. Lett.* **1991**, 181, 319.
- (20) Häser, M.; Almlöf, J. *J. Chem. Phys.* **1992**, 96, 489.
- (21) Möller, C.; Plesset, M. S. *Phys. Rev.* **1934**, 46, 618.
- (22) Ayala, P. Y.; Scuseria, G. E. *J. Chem. Phys.* **1999**, 110, 3660.
- (23) Ayala, P. Y.; Kudin, K. N.; Scuseria, G. E. *J. Chem. Phys.* **2001**, 115, 9698.
- (24) Kats, D.; Usvyat, D.; Schütz, M. *Phys. Chem. Chem. Phys.* **2008**, 10, 3430.
- (25) Izmaylov, A. F.; Scuseria, G. E. *Phys. Chem. Chem. Phys.* **2008**, 10, 3421.
- (26) Grimme, S. *J. Chem. Phys.* **2003**, 118, 9095.
- (27) Grimme, S.; Izgorodina, E. I. *Chem. Phys.* **2004**, 305, 223.
- (28) Szabados, A. *J. Chem. Phys.* **2006**, 125, 214105.
- (29) Jung, Y.; Lochan, R. C.; Dutoi, A. D.; Head-Gordon, M. *J. Chem. Phys.* **2004**, 121, 9793.
- (30) Rhee, Y. M.; Head-Gordon, M. *J. Phys. Chem. A* **2007**, 111, 5314.
- (31) Head-Gordon, M.; Rico, R. J.; Oumi, M.; Lee, T. J. *Chem. Phys. Lett.* **1994**, 219, 21.
- (32) Casanova, D.; Rhee, Y. M.; Head-Gordon, M. *J. Chem. Phys.* **2008**, 128, 164106.
- (33) Head-Gordon, M.; Oumi, M.; Maurice, D. *Mol. Phys.* **1999**, 96, 593.
- (34) Hellweg, A.; Grun, S. A.; Hättig, C. *Phys. Chem. Chem. Phys.* **2008**, 10, 4119.
- (35) Christiansen, O.; Koch, H.; Jørgensen, P. *Chem. Phys. Lett.* **1995**, 243, 409.
- (36) Lochan, R. C.; Shao, Y. H.; Head-Gordon, M. *J. Chem. Theory Comput.* **2007**, 3, 988.
- (37) Casida, M. E.; Gutierrez, F.; Guan, J.; Gadea, F.-X.; Salahub, D.; Daudey, J.-P. *J. Chem. Phys.* **2000**, 113, 7062.
- (38) Dreuw, A.; Head-Gordon, M. *J. Am. Chem. Soc.* **2004**, 126, 4007.
- (39) Neugebauer, J.; Gritsenko, O.; Baerends, E. J. *J. Chem. Phys.* **2006**, 124, 214101.
- (40) Hieringer, W.; Görling, A. G. *Chem. Phys. Lett.* **2006**, 419, 557.
- (41) Dreuw, A.; Head-Gordon, M. *Chem. Phys. Lett.* **2006**, 426, 231.
- (42) Hieringer, W.; Görling, A. G. *Chem. Phys. Lett.* **2006**, 426, 234.
- (43) Izmaylov, A. F.; Scuseria, G. E. *J. Chem. Phys.* **2008**, 129, 034101.
- (44) DiStasio Jr, R. A.; Steele, R. P.; Rhee, Y. M.; Shao, Y.; Head-Gordon, M. *J. Comput. Chem.* **2007**, 28, 839.
- (45) Maurice, D.; Head-Gordon, M. *Mol. Phys.* **1999**, 96, 1533.
- (46) Foresman, J. B.; Head-Gordon, M.; Pople, J. A.; Frisch, M. J. *J. Phys. Chem.* **1992**, 96, 135.
- (47) Aikens, C. M.; Webb, S. P.; Bell, R. L.; Fletcher, G. D.; Schmidt, M. W.; Gordon, M. S. *Theor. Chem. Acc.* **2003**, 110, 233.
- (48) Szabo, A.; Ostlund, N. S. *Modern Quantum Chemistry: Introduction to Advanced Electronic Structure Theory*; McGraw-Hill: New York, 1989.
- (49) Pulay, P. *Mol. Phys.* **1969**, 17, 197.
- (50) Handy, N. C.; Amos, R. D.; Gaw, J. F.; Rice, J. E.; Simandrias, E. D. *Chem. Phys. Lett.* **1985**, 120, 151.
- (51) Head-Gordon, M. *Mol. Phys.* **1999**, 96, 673.
- (52) Rhee, Y. M.; DiStasio, R. A., Jr.; Lochan, R. C.; Head-Gordon, M. *Chem. Phys. Lett.* **2006**, 426, 197.
- (53) Handy, N. C.; Schaefer, H. F. *J. Chem. Phys.* **1984**, 81, 503.
- (54) Frisch, M. J.; Head-Gordon, M.; Pople, J. A. *Chem. Phys. Lett.* **1990**, 166, 281.
- (55) Frisch, M. J.; Head-Gordon, M.; Pople, J. A. *Chem. Phys. Lett.* **1990**, 166, 275.
- (56) Yamaguchi, Y.; Goddard, J. D.; Osamura, Y.; Schaefer, H. F., III *A New Dimension to Quantum Chemistry: Analytic Derivative Methods in Ab Initio Molecular Electronic Structure Theory*; Oxford University Press: New York, 1994.
- (57) Shao, Y.; Molnar, L. F.; Jung, Y.; Kussmann, J.; Ochsenfeld, C.; Brown, S. T.; Gilbert, A. T. B.; Slipchenko, L. V.; Levchenko, S. V.; O'Neill, D. P.; DiStasio, R. A.; Lochan, R. C.; Wang, T.; Beran, G. J. O.; Besley, N. A.; Herbert, J. M.; Lin, C. Y.; van Voorhis, T.; Chien, S. H.; Sodt, A.; Steele, R. P.; Rassolov, V. A.; Maslen, P. E.; Korambath, P. P.; Adamson, R. D.; Austin, B.; Baker, J.; Byrd, E. F. C.; Dachsel, H.; Doerksen, R. J.; Dreuw, A.; Dunietz, B. D.; Dutoi, A. D.; Furlani, T. R.; Gwaltney, S. R.; Heyden, A.; Hirata, S.; Hsu, C.-P.; Kedziora, G.; Khallullin, R. Z.; Klunzinger, P.; Lee, A. M.; Lee, M. S.; Liang, W.; Lotan, I.; Nair, N.; Peters, B.; Proynov, E. I.; Pieniazek, P. A.; Rhee, Y. M.; Ritchie, J.; Rosta, E.; Sherrill, C. D.; Simmonett, A. C.; Subotnik, J. E.; Woodcock, H. L., III; Zhang, W.; Bell, A. T.; Chakraborty, A. K.; Chipman, D. M.; Keil, F. J.; Warshel, A.; Hehre, W. J.; Schaefer, H. F., III; Kong, J.; Krylov, A. I.; Gill, P. M. W.; Head-Gordon, M. *Phys. Chem. Chem. Phys.* **2006**, 8, 3172.
- (58) Kendall, R. A.; Dunning, T. H.; Harrison, R. J. *J. Chem. Phys.* **1992**, 96, 6796.
- (59) Weigend, F.; Köhn, A.; Hättig, C. *J. Chem. Phys.* **2002**, 116, 3175.